

Boltzmann test of Slonczewski's theory of spin-transfer torque

Jiang Xiao and A. Zangwill

School of Physics, Georgia Institute of Technology, Atlanta, Georgia 30332-0430, USA

M. D. Stiles

Electron Physics Group, National Institute of Standards and Technology, Gaithersburg, Maryland 20899-8412, USA

(Received 21 July 2004; published 12 November 2004)

We use a matrix Boltzmann equation formalism to test the accuracy of Slonczewski's theory of spin-transfer torque in thin-film heterostructures where a nonmagnetic spacer layer separates two noncollinear ferromagnetic layers connected to nonmagnetic leads. When applicable, the model predictions for the torque as a function of the angle between the two ferromagnets agree extremely well with the torques computed from a Boltzmann equation calculation. We focus on asymmetric structures (where the two ferromagnets and two leads are not identical) where the agreement pertains to an analytic formula for the torque derived by us using Slonczewski's theory. In almost all cases, we can predict the correct value of the model parameters directly from the geometric and transport properties of the multilayer. For some asymmetric geometries, we predict a mode of stable precession that does not occur for the symmetric case studied by Slonczewski.

DOI: 10.1103/PhysRevB.70.172405

PACS number(s): 75.47.-m, 75.70.Cn

In 1996, Slonczewski¹ and Berger² predicted that an electric current flowing through a magnetic multilayer can exert a spin-transfer torque on the magnetic moments of the heterostructure. This torque can produce stable magnetic precession and/or magnetic reversal, both of which have been widely studied experimentally³ and theoretically.⁴ Figure 1 illustrates a common geometry known as a "spin valve," where a nonmagnetic spacer layer separates a thick "pinned" ferromagnetic layer from a thin "free" ferromagnetic layer. Nonmagnetic leads connect the ferromagnets to electron reservoirs.

Slonczewski⁵ developed a theory of spin-transfer torque that combines a density-matrix description of the spacer layer with a circuit theory⁶ description of the remainder of the structure. He worked out the algebra for the case where the spacer layer is thin and the spin valve is symmetric (identical ferromagnets and leads), and found the torque L_S to be the same on the left and right spacer/ferromagnet interfaces. As a function of the angle between the two ferromagnets,

$$L_S(\theta) = \frac{\hbar I}{2e} \frac{P \Lambda^2 \sin \theta}{(\Lambda^2 + 1) + (\Lambda^2 - 1) \cos \theta}. \quad (1)$$

In this formula, I is the total current that flows through the structure,

$$P = \frac{\frac{1}{2}(R_\downarrow - R_\uparrow)}{\frac{1}{2}(R_\downarrow + R_\uparrow)} = \frac{r}{R} \text{ and } \Lambda^2 = GR. \quad (2)$$

R_\uparrow and R_\downarrow are *effective* resistances experienced by spin-up and spin-down electrons between the reservoir and the spacer layer. The conductance $G = Se^2 k_F^2 / 4\pi^2 \hbar$, where k_F is the Fermi wave vector and S is the cross-sectional area of the device.⁷

In this paper, we solve Slonczewski's equations for the general asymmetric case and derive formulas for the torques $L_L(\theta)$ and $L_R(\theta)$ on the left ($x=x_L$) and right ($x=x_R$) spacer/ferromagnet interfaces in Fig. 1. We then compare these formulas with numerical results for the torque obtained from a matrix Boltzmann equation.⁸ From this comparison, we are

able to identify the physical origin and systematic behavior of the effective resistances R_\uparrow and R_\downarrow in the interplay between resistive scattering, spin-flip scattering, and interface scattering. For some asymmetric geometries, a previously unsuspected feature of the torque leads us to predict a mode of stable precession that does not occur for the symmetric case.

The electric current in the real, physical spin valve can be written as the sum of spatially varying currents carried by up and down⁹ spin electrons: $I = I_\uparrow(x) + I_\downarrow(x)$. The corresponding spin current¹⁰ is $\Delta I(x) = I_\downarrow(x) - I_\uparrow(x)$. The up and down spin voltage (chemical potential) drops along the spin valve are $V_\uparrow(x)$ and $V_\downarrow(x)$. Slonczewski⁵ contracted the function $I_\uparrow(x)$ to the values $I_\uparrow^L = I_\uparrow(x_L)$ and $I_\uparrow^R = I_\uparrow(x_R)$ and similarly for $I_\downarrow(x)$. He also writes $\Delta V_R = V_\uparrow(x_R) - V_\downarrow(x_R)$ for the up-down difference in the voltage drop from the right reservoir to a point in the spacer infinitesimally close to the interface between the spacer and the right ferromagnet. ΔV_L is defined similarly. These quantities are directly proportional to the spin accumulation at x_R and x_L , respectively.

With this model, Slonczewski wrote down (but did not completely solve) all the equations needed for the asymmetric geometry. In our notation, two of his linear equations relate the voltage drop differences to the spin currents,

$$0 = \Delta V_L (1 + \cos^2 \theta) - G^{-1} \Delta I_L \sin^2 \theta - 2 \Delta V_R \cos \theta,$$

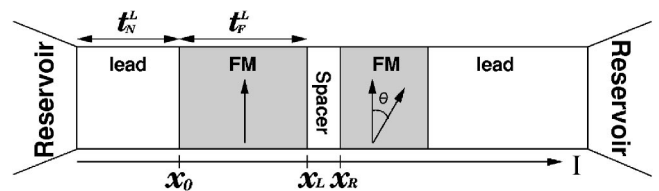


FIG. 1. Schematic of a five-layer spin valve. A nonmagnetic spacer layer separates two ferromagnetic layers whose magnetizations are inclined from one another by an angle θ . A nonmagnetic lead connects each ferromagnet to an electron reservoir.

$$0 = \Delta I_L(1 + \cos^2 \theta) - G\Delta V_L \sin^2 \theta - 2\Delta I_R \cos \theta. \quad (3)$$

Two additional equations parametrize the voltage drop differences in terms of effective resistances R_L , R_R , r_L , and r_R :

$$\begin{aligned} \Delta V_L &= \Delta I_L R_L + I r_L, \\ \Delta V_R &= -\Delta I_R R_R - I r_R. \end{aligned} \quad (4)$$

Finally, Slonczewski derived expressions for the interfacial torques. At $x=x_R$, the torque is

$$L_R = \frac{\hbar}{2e} \frac{\Delta I_R \cos \theta - \Delta I_L}{\sin \theta}. \quad (5)$$

The torque L_L at the $x=x_L$ interface is (5) with ΔI_R and ΔI_L exchanged.

It is straightforward to solve the four equations (3) and (4) for the four unknowns, ΔI_L , ΔI_R , ΔV_L , and ΔV_R . From these, we find L_R from (5) to be

$$L_R = \frac{\hbar}{2e} I \sin \theta \left[\frac{q_+}{A + B \cos \theta} + \frac{q_-}{A - B \cos \theta} \right], \quad (6)$$

where

$$\begin{aligned} q_{\pm} &= \frac{1}{2} \left[P_L \Lambda_L^2 \sqrt{\frac{\Lambda_R^2 + 1}{\Lambda_L^2 + 1}} \pm P_R \Lambda_R^2 \sqrt{\frac{\Lambda_L^2 - 1}{\Lambda_R^2 - 1}} \right], \\ A &= \sqrt{(\Lambda_L^2 + 1)(\Lambda_R^2 + 1)}, \\ B &= \sqrt{(\Lambda_L^2 - 1)(\Lambda_R^2 - 1)}. \end{aligned} \quad (7)$$

The parameters P_L , P_R , Λ_L , and Λ_R are defined in terms of R_L , R_R , r_L , and r_R as P and Λ are defined in (2) in terms of R and r . For the symmetric case, $\Lambda_L = \Lambda_R = \Lambda$ and $P_L = P_R = P$. This makes $q_- = 0$ and (6) reduces to Slonczewski's formula (1) with $L_R = L_L = L_S$. We will see later that the term proportional to q_- in (6) can affect the magnetization dynamics of the spin valve in a qualitative way.

To test (6), we computed the torque on each spacer/ferromagnet interface using a Boltzmann equation formalism.⁸ The two ferromagnetic moments in Fig. 1 are not collinear, so there is no natural spin quantization axis in the spacer layer. Therefore, we expand the deviation of the semiclassical electron occupation function from its equilibrium value in a basis of Pauli spin matrices,

$$\begin{aligned} \mathbf{g}(\mathbf{k}, \mathbf{r}) &= g_0(\mathbf{k}, \mathbf{r}) \begin{pmatrix} 1 & 0 \\ 0 & 1 \end{pmatrix} + g_x(\mathbf{k}, \mathbf{r}) \begin{pmatrix} 0 & 1 \\ 1 & 0 \end{pmatrix} + g_y(\mathbf{k}, \mathbf{r}) \begin{pmatrix} 0 & -i \\ i & 0 \end{pmatrix} \\ &+ g_z(\mathbf{k}, \mathbf{r}) \begin{pmatrix} 1 & 0 \\ 0 & -1 \end{pmatrix}. \end{aligned} \quad (8)$$

In the spacer layer, each of g_0 , g_x , g_y , and g_z satisfies a linear Boltzmann equation that takes account of the driving current and of resistive and spin-flip scattering in each material layer. In each ferromagnet and in the adjacent lead, it is sufficient to use g_0 and g_z referenced to the fixed direction of magnetization in each. We assume a spherical Fermi surface for each material. We adopt a one-dimensional approximation $\mathbf{g}(\mathbf{k}, \mathbf{r}) = \mathbf{g}(\mathbf{k}, x)$ and stitch together the solutions in each

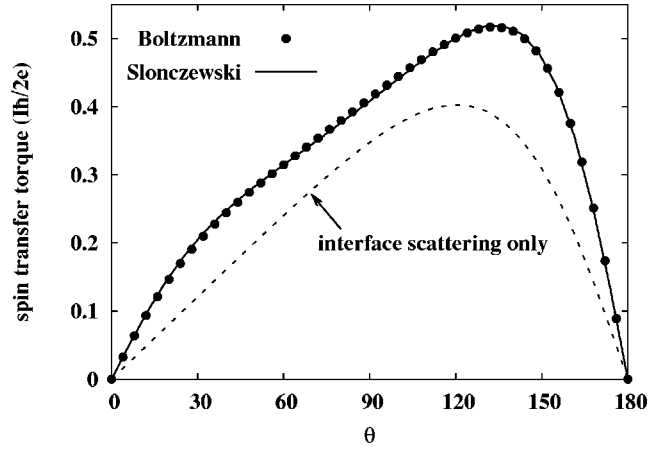


FIG. 2. Spin-transfer torque at $x=x_R$ for a spin valve with layer thicknesses 5 nm/40 nm/1 nm/180 nm. Solid circles are Boltzmann equation results. The solid curve is Eq. (6) derived from Slonczewski's theory. The dashed curve is Eq. (6) with all bulk scattering removed.

layer with matching conditions that reflect the complex, spin- and wave-vector-dependent reflection and transmission amplitudes of each interface. The latter are determined from a previously published parametrization.¹¹

Electrons that enter a nonmagnetic lead from the adjacent reservoir are assumed to have an equilibrium occupation function. For our numerical work, we have chosen material and geometry parameters typical of experiments performed on Cu/Co/Cu/Co/Cu spin valves. The specific numerical values used can be found in Ref. 8. With the final occupation function in hand, it is straightforward to compute the spatially varying voltage, spin accumulation, spin current, and spin-transfer torque. Details will be published elsewhere.¹²

The filled circles in Fig. 2 show a typical Boltzmann result for the spin-transfer torque at $x=x_R$ as a function of the angle θ between the two ferromagnets for an asymmetric geometry. The solid curve in Fig. 2 is the same quantity, $L_R(\theta)$, computed from (6). The agreement is excellent, as it is for essentially all other geometries we have studied with thin spacer layers. For comparison, the dashed curve is the Slonczewski torque (6) with the bulk scattering removed. This “interface-only” situation is manifestly symmetric ($q_- = 0$).

For the solid curve plotted in Fig. 2, the relative importance of the two terms in (6) is $q_-/q_+ \approx 0.27$. We find that this ratio does not exceed about 0.5 for physically sensible geometries. We will address the qualitative consequences of $q_- \neq 0$ at the end. First, we describe our method to determine the torque parameters Λ_R , Λ_L , P_R , and P_L that produced the solid curve in Fig. 2. We begin by writing an exact expression for the voltage drop difference ΔV_L in (4),

$$\Delta V_L = \int_{-\infty}^{x_L} dx [I_{\downarrow}(x)\rho_{\downarrow}(x) - I_{\uparrow}(x)\rho_{\uparrow}(x)]. \quad (9)$$

The average resistivity (used below) is $\bar{\rho} = (\rho_{\uparrow} + \rho_{\downarrow})/2$. We will also need the resistivity difference $\Delta\rho = (\rho_{\downarrow} - \rho_{\uparrow})/2$. Both $\bar{\rho}$ and $\Delta\rho$ contain delta functions at the four nonmagnet/ferromagnet interfaces to take account of spin-dependent interface scattering.

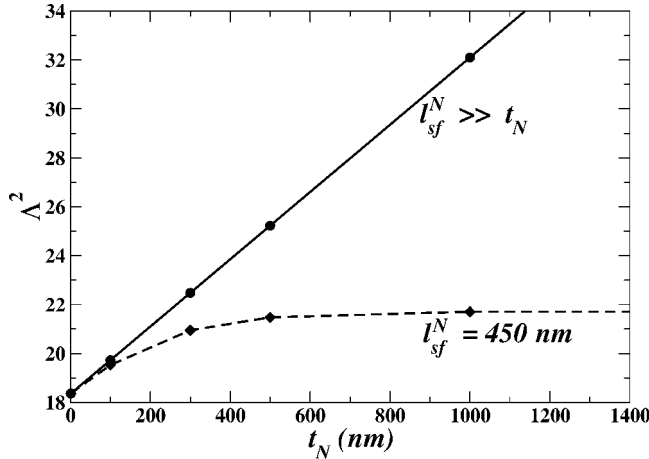


FIG. 3. Torque parameter Λ^2 as a function of t_N for large and small values of l_{sf}^N .

To make progress, we use a drift-diffusion result¹³ to the effect that close to the outer $x=x_0$ interface (Fig. 1), $I_{\uparrow}(x)$ and $I_{\downarrow}(x)$ approach the corresponding bulk values exponentially in both directions. The decay length is the spin-flip length in each material, whether ferromagnet (F) or nonmagnet (N). In that case, an approximate expression for (9) is

$$\Delta V_L = \Delta I_0 \bar{\rho}_N d_N^L + \Delta I_0 \bar{\rho}_F d_F^L + I \Delta \rho_F d_F^L + \Delta V_I + \Delta V_C. \quad (10)$$

In Eq. (10), $\Delta I_0 = \Delta I(x_0)$, ΔV_I and ΔV_C are voltage drops at the internal interfaces and at the reservoir contact, and

$$d_F^L = l_{sf}^F [1 - \exp(-t_F^L/l_{sf}^F)],$$

$$d_N^L = l_{sf}^N [1 - \exp(-t_N^L/l_{sf}^N)]. \quad (11)$$

The effective lengths (11) appear because, due to spin-flip scattering, only electrons within d_F or d_N of the ferromagnetic interfaces can accommodate the dissimilar spin-currents characteristic of the ferromagnets and the nonmagnets in equilibrium.

The relationship between ΔI_0 and ΔI_L is nontrivial¹³ except when the ferromagnet is very thin ($t_F^L \ll l_{sf}^F$). In that case,

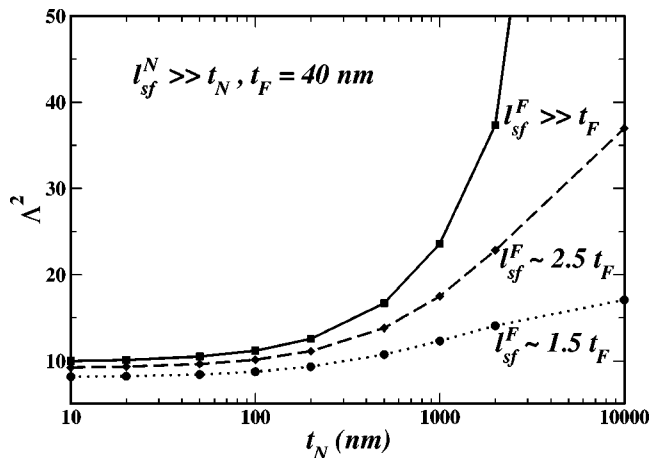
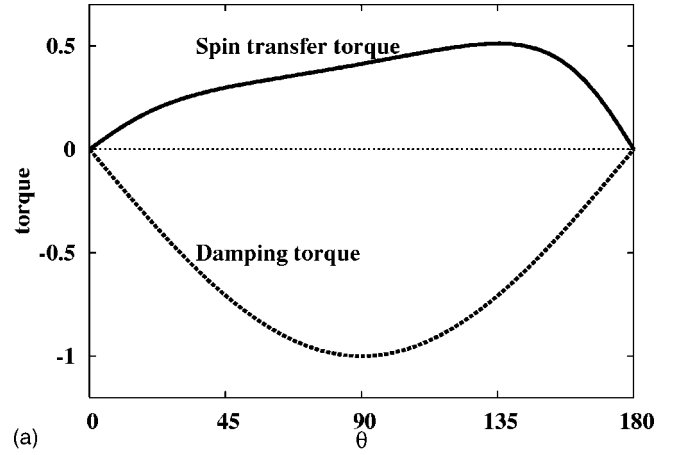
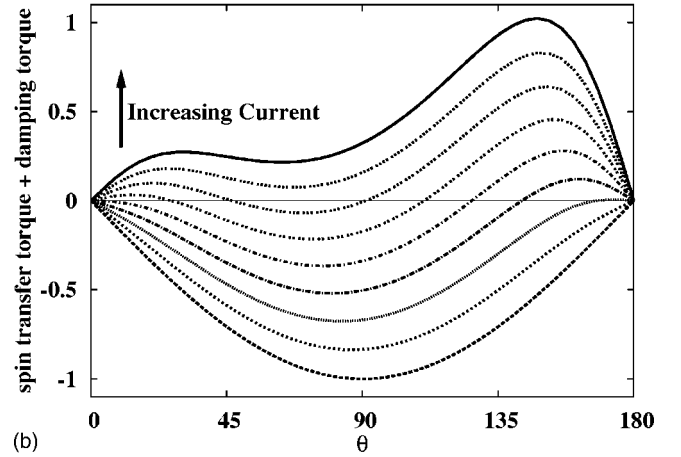


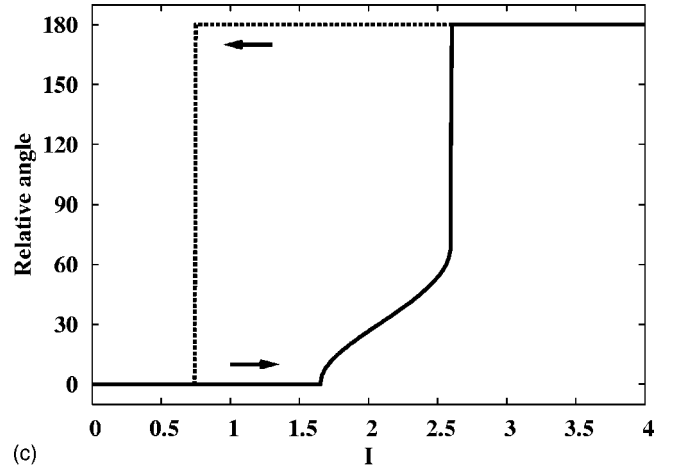
FIG. 4. Torque parameter Λ^2 as a function of t_N for different values of l_{sf}^F . In all cases, $l_{sf}^N = \infty$. The curve for $l_{sf}^F \gg t_F$ corresponds to $\Lambda^2 \propto t_N$.



(a)



(b)



(c)

FIG. 5. Left: Spin-transfer torque and damping torque for a 1 nm/40 nm/1 nm/1000 nm spin valve ($q_-/q_+ \approx 0.36$). Middle: the total torque as the current increases. Right: the angle between two ferromagnetic moments as a function of current I in arbitrary units.

$\Delta I_0 \approx \Delta I_L$, and we can connect (10) to (4) and (6) to get

$$\Lambda_L^2 = G(\bar{\rho}_N d_N^L + \bar{\rho}_F t_F^L + \bar{R}_I + \bar{R}_C),$$

$$P_L = G\Lambda_L^{-2}(\Delta \rho_F t_F^L + \Delta R_I). \quad (12)$$

These two formulas (and similar ones for Λ_R and P_R), together with (6) and (7) are the principal results of this paper. We used (12) to compute the solid curve in Fig. 2. The in-

interface resistance $GR_I \approx 0.97$ and contact resistance $GR_C \approx 1.1$ were extracted from the Boltzmann solution. GR_I differs from the experimental value by about 15%.¹⁴

The parametrization (6) is well suited to study the behavior of $L(\theta)$ when we vary the geometry of the magnetic heterostructure and the material parameters in our Boltzmann calculations. Related calculations of the angular dependence of the torque for asymmetric geometries have been performed by Manschot *et al.*¹⁵ For simplicity, we focus on symmetric geometries in what follows. Figure 3 confirms that Λ^2 is a linear function of t_N when $l_{sf}^N \gg t_N$ but saturates when $t_N \sim l_{sf}^N$. Interestingly, the saturated value of Λ^2 varies linearly with $l_{sf}^N - l^N$ (l^N is the inelastic scattering length) rather than with l_{sf}^N as predicted by (11). For long leads, this can be understood from the fact that conventional resistive scattering is needed to build up nonequilibrium spin accumulation in the nonmagnet while spin-flip scattering works to return the nonmagnet to equilibrium.

Figure 4 shows the variation of Λ^2 with lead length for different values of the spin-flip length in the ferromagnet. This calculation puts $l_{sf}^N \rightarrow \infty$, so we expect from (11) that $\Lambda^2 \propto t_N$. This is indeed the case when $l_{sf}^F \gg l^F$. However, when the l_{sf}^F is comparable (or less than) the ferromagnetic layer thickness, the torque parameter saturates. This is a signal that our approximation $\Delta I_0 \approx \Delta I_L$ has broken down. In this limit, fast spin-flipping in the ferromagnet reduces ΔI_0 to a value much less than ΔI_L . When that is the case, relatively little spin-flip volume in the nonmagnet is needed to reduce the spin current in the nonmagnet to zero (its equilibrium value).

A characteristic difference between $L_S(\theta)$ in (1) for a symmetric geometry and $L_R(\theta)$ in (6) for an asymmetric geom-

etry can be seen from the difference between the dashed curve and the solid curve in Fig. 2. The former has a bump (maximum) in the interval $\pi/2 < \theta < \pi$ only. The latter has a small additional bump in the interval $0 < \theta < \pi/2$ that comes from the q_- term.¹⁶ This small change is enough to produce stable magnetization precession for some asymmetric geometries.

Consider a spin valve in the presence of an external magnetic field aligned with the magnetization of the thick ferromagnet. If we ignore shape anisotropy and lattice anisotropy, the total torque acting on the thin ferromagnetic film when electrons flow from right to left in Fig. 1 is the sum of the spin-transfer torque $L_R(\theta)$ and a Gilbert damping torque $\gamma H \sin \theta$ (left panel of Fig. 5). As the current increases, the spin-transfer torque increases and eventually destabilizes an initial state with parallel moments. Stable precession occurs at angles where the total torque changes from positive to negative (middle panel of Fig. 5). When the total torque becomes everywhere positive, the system abruptly switches to the anti-parallel configuration (right panel of Fig. 5). There is no regime of stable precession if the zero-current state is antiparallel.¹⁷

In summary, we have shown that Slonczewski's theory of spin-transfer torque in spin valves can reproduce the results of Boltzmann equation calculations when the nonmagnetic spacer layer is thin. When the ferromagnetic layers are also thin, the parameters of the theory can be calculated from first principles.

One of us (J.X.) acknowledges support from the National Science Foundation under Grant No. DMR-9820230.

¹J. C. Slonczewski, J. Magn. Magn. Mater. **159**, L1 (1996).

²L. Berger, Phys. Rev. B **54**, 9353 (1996).

³J. A. Katine, F. J. Albert, and R. A. Buhrman, E. B. Myers, and D. C. Ralph, Phys. Rev. Lett. **84**, 3149 (2000); S. Urazhdin, N. O. Birge, W. P. Pratt, and J. Bass, *ibid.* **91**, 146803 (2003); W.H. Rippard, M.R. Pufall, S. Kaka, S.E. Russek, and T.J. Silva, *ibid.* **92**, 027201 (2004); A. Fert, V. Cros, J.-M. George, J. Grollier, H. Jaffrès, A. Hamzic, A. Vaurès, G. Faini, J. Ben Youssef, and H. Le Gail, J. Magn. Magn. Mater. **272–276**, 1706 (2004).

⁴J. Z. Sun, Phys. Rev. B **62**, 570 (2000); D. H. Hernando, Yu. V. Nazarov, A. Brataas, and G. E.W. Bauer, *ibid.* **62**, 5700 (2000); X. Waintal, E. B. Myers, P. W. Brouwer, and D. C. Ralph, *ibid.* **62**, 12317 (2000); M. D. Stiles and A. Zangwill, *ibid.* **66**, 014407 (2002); Z. Li and S. Zhang *ibid.* **68**, 024404 (2003); Ya. B. Bazaliy, B. A. Jones, and Shou-Cheng Zhang, *ibid.* **66**, 094421 (2004).

⁵J. C. Slonczewski, J. Magn. Magn. Mater. **247**, 324 (2002).

⁶A. Brataas, Y. V. Nazarov, and G. E. W. Bauer, Eur. Phys. J. B **22**, 99 (2001).

⁷For Cu, $S/G=0.878$ f Ω m².

⁸M. D. Stiles and A. Zangwill, J. Appl. Phys. **91**, 6812 (2002).

⁹In the each ferromagnet (and in the adjacent nonmagnetic lead), we use the magnetization direction of the ferromagnet to define “up” and “down.”

¹⁰The spin current $Q_{\alpha\beta}$ is a second rank tensor. Here, we need only one spatial index (the direction of current flow) and one spin index (the local direction of spin polarization), so a scalar ΔI is sufficient.

¹¹M. D. Stiles and D. R. Penn, Phys. Rev. B **61**, 3200 (2000).

¹²J. Xiao, M. Stiles, and A. Zangwill (unpublished).

¹³M. D. Stiles, J. Xiao, and A. Zangwill, Phys. Rev. B **69**, 054408 (2004). We have also calculated $L_R(\theta)$ using the drift-diffusion formalism described in this paper. The agreement with Boltzmann is only qualitative.

¹⁴The relationship between the Boltzmann and experimental values for R_I is not straightforward, (Ref. 12). The experimental values are accurate to 10%–20% [Jack Bass (private communication)].

¹⁵J. Manschot, A. Brataas, and G. E. W. Bauer, Phys. Rev. B **69**, 092407 (2004); cond-mat/0403760; Phys. Rev. B (to be published).

¹⁶Slonczewski (Ref. 5) notes that the single bump in $L_S(\theta)$ moves from $\pi/2 < \theta < \pi$ to $0 < \theta < \pi/2$ as the coefficient of $\cos \theta$ in (1) changes sign as a function of Λ .

¹⁷The anisotropy-driven precession state found by Bazaliy *et al.* in Ref. 4 using Eq. (1) occurs only when the magnetization and the external field are nearly antiparallel.